LETTER

Chaotic Detection of Target Signal in HFSWR Ionospheric Clutter Background under Typhoon Excitation

Rong WANG[†a)], **Changjun YU**[†b)], **Zhe LYU**[†c)], *and* **Aijun LIU**[†d)], *Nonmembers*

SUMMARY To address the challenge of target signals being completely submerged by ionospheric clutter during typhoon passages, this letter proposes a chaotic detection method for target signals in the background of ionospheric noise under typhoon excitation. Experimental results demonstrate the effectiveness of the proposed method in detecting target signals with harmonic characteristics from strong ionospheric clutter during typhoon passages.

key words: *high-frequency radar, target detection, ionospheric clutter, chaos, typhoon*

1. Introduction

High-Frequency Surface Wave Radar (HFSWR) stands out as an emerging marine surveillance technology of significant military strategic importance in national maritime defense fortification [1]. The distribution of ionospheric clutter exhibits characteristics such as time variation, wide coverage, and non-stationarity, playing a predominant role in HFSWR clutter interference and emerging as a primary limitation on the detection performance of maritime targets [2]. In particular, during typhoons, the dynamic behavior of the ionosphere becomes even more unpredictable. Substantial progress has been made in recent years regarding HFSWR clutter suppression. However, various clutter suppression methods in HFSWR still have their limitations and cannot perfectly suppress ionospheric clutter signals while preserving target signals. Effectively suppressing ionospheric clutter and accurately detecting targets remain a challenge.

In 1960, Hines and others first proposed the use of gravity wave theory to explain the disturbance of the ionosphere caused by severe weather phenomena such as typhoons, thunderstorms, and tornadoes [3]. Researchers have observed quasi-periodic sinusoidal "S"-shaped traveling ionospheric disturbances (TIDs) in ionospheric echoes using various detection devices, confirming that gravity waves excited by typhoons can propagate into the ionosphere, triggering TIDs. There exists a physical mechanism linking typhoons and the ionosphere [4].

Chaos theory, as a novel approach to studying nonlinear systems, has been widely researched and has shown significant breakthroughs in the analysis and investigation of complex clutter backgrounds, target detection and estimation, and the development of new theories. Brix and Pipenberg utilized chaotic oscillators to detect signals submerged in white noise. In 1998, Leung explored the immune characteristics of chaotic systems to noise and their sensitivity to target signals [5]. By utilizing the chaotic transition to the periodic state, Leung achieved target signal detection in the presence of strong noise backgrounds [6]. Lyu et al. demonstrated the chaotic nature of ionospheric echoes using actual HFSWR ionospheric data and proposed corresponding chaotic prediction models [7], which provide novel insights for target signal detection in the presence of strong ionospheric backgrounds in HFSWR.

Dual-coupled Duffing chaotic system has been widely applied in various signal detection and recovery applications due to its stronger noise resistance, more stable phase variation, and more complex dynamics, which allow for the utilization of multiple states more easily [8]. Therefore, this study combines the sensitivity of the Duffing chaotic system to weak signals and the non-chaotic nature of target signals, employing the phase transition characteristics of the Duffing chaotic system to achieve target signal detection within the strong ionospheric background clutter under gravity wave excitation based on HFSWR. This breakthrough contributes to the field of HFSWR target detection.

2. Chaos Detection Method of HFSWR Target Signal Based on Dual-Coupled Duffing Oscillator

This letter adopts the principle of forward detection. Firstly, the dual-coupled Duffing oscillator is adjusted to the critical chaotic state. Furthermore, the target signal, $s(t)$, is injected into the double-coupled Duffing oscillator system, where its amplitude interacts with the parameter A, resulting in a total driving force. When the total driving force exceeds the critical threshold A_c, the phase diagram transitions from a chaotic state to large-scale periodic motion, indicating the presence of a weak target signal in the detected signal. Otherwise, the detected signal only contains ionospheric clutter signals with chaotic properties [9]. The first issue to address is how to quickly and accurately identify whether the oscillator system transitions from a chaotic motion state to a large-scale periodic state. There are typical methods to discern chaotic systems, namely intuitive methods and quantitative methods. Among them, the subjective nature of determining the

Manuscript received December 16, 2023.
Manuscript revised April 10, 2024.
Manuscript publicized May 23, 2024.

[†]College of Information Science and Engineering, Harbin Institute of Technology, Weihai 264209, China.
a) E-mail: wangrongrong312@163.com
b) E-mail: yuchangjun@hit.edu.cn
c) E-mail: lvzhehit@126.com
d) E-mail: liuaijun@hit.edu.cn

DOI: 10.1587/transfun.2023EAL2109

change in the chaotic oscillator motion state by observing the phase diagram is strong. The estimation of the phase diagram becomes blurred under the influence of strong noise, leading to potential misjudgment of the actual motion state of the Duffing oscillator. Minkowski distance can reflect the ordered properties of a set of N-dimensional spatial data. In this research, a modified version of Minkowski distance is employed to quantitatively describe the chaotic level of the time series of chaotic oscillators and differentiate the phase transition of the Duffing oscillator.

2.1 Dual-Coupled Duffing Oscillator

Dual-coupled Duffing oscillator utilizes two Duffing oscillators to connect and control each other, which improves the system's stability at the critical bifurcation. The mathematical description of the dual-coupled Duffing oscillator is as follows [10],

$$\begin{cases} \frac{1}{\omega^2}\ddot{x} + \frac{k}{\omega}\dot{x} - x + mx(x^2+y^2) &= A\cos(\omega t) + s(t) \\ \frac{1}{\omega^2}\ddot{y} + \frac{k}{\omega}\dot{y} - y + my(x^2+y^2) &= A\sin(\omega t) + s(t) \end{cases} \tag{1}$$

where, $A\cos(\omega t)$ denotes cyclical momentum, $\frac{k}{\omega}$ is damping ratio, m represents the coupling coefficient. $s(t)$ is an external signal source corresponding to the experimental data in Sect. 3. When $y = 0$, the system is a single coupled Duffing oscillator. The study of the system response of the dual-coupled form of Duffing is more general and possesses broader practical significance. Let $x_1 = x, x_2 = \frac{\dot{x}}{\omega}, x_3 = y, x_4 = \frac{\dot{y}}{\omega}$, then the double-coupled Duffing oscillator equation becomes,

$$\begin{cases} \dot{x_1} = \omega x_2 \\ \dot{x_2} = \omega\left[x_1 - kx_2 - mx_1\left(x_1^2 + x_3^2\right) + A\cos(\omega t) + s(t)\right] \\ \dot{x_3} = \omega x_4 \\ \dot{x_4} = \omega\left[x_3 - kx_4 - mx_3\left(x_3^2 + x_1^2\right) + A\sin(\omega t) + s(t)\right] \\ \dot{\theta} = 1; m, k, w, A > 0 \end{cases} \tag{2}$$

This letter uses the Rungekutta method to solve (2). The phase diagram $(x_1, \dot{x}_1)$ is used as the output term of the system. Combining Duffing output phase diagrams of various driving signals to study the Duffing system's response characteristics of the HFSWR ocean-ionosphere joint gravity wave signals.

2.2 HFSWR Phase Transition Criterion based on Duffing Oscillator

Euclidean distance from any point $(x_i, \dot{x}_i)$ in the phase image to the start point (0,0) is [11], [12],

$$d_{i0} = \sqrt{x_i^2 + \dot{x}_i^2} \tag{3}$$

It is necessary to evaluate the order of a two-dimensional phase image accurately. Accordingly, in this letter, the evaluation index of the image order is the average of Euclidean distances from all points in the two-dimensional phase image to the starting point. This letter defines the average Euclidean distance of the phase diagram of a dual-coupled Duffing oscillator to be the,

$$d_{sj}(X,Y) = \frac{1}{N}\sum_{j=1}^{N}\sqrt{\sum_{s=1}^{M}\left(X_{sj}^2 + Y_{sj}^2\right)} \tag{4}$$

where $s = 1, 2, \ldots, M$, M denotes the number of phase diagrams to be recognized. $X_{sj}(j = 1, 2, \ldots, N)$ denotes the jth value of the horizontal coordinate of the sth phase diagram, $Y_{sj}(j = 1, 2, \ldots, N)$ denotes the jth value of the vertical coordinate of the sth phase diagram, N is the data length.

The degree of dispersion undergoes a jump during the phase transition in the dual-coupled Duffing system. Consequently, this letter utilizes the standard deviation method to weight the average Euclidean distance to quantitatively identify the extent of chaos in the motion state of the Duffing oscillator.

$$\begin{aligned} \mathrm{HPTC_s} = \sigma_{\mathrm{X_s}} \times \sigma_{\mathrm{Y_s}} \times \mathrm{d_s} = \frac{1}{\mathrm{N}}\sum_{\mathrm{j=1}}^{\mathrm{N}}\sqrt{\left(\mathrm{X_{sj}} - \overline{\mathrm{X}}_{\mathrm{s}}\right)^2} \\ \times \frac{1}{N}\sum_{j=1}^{N}\sqrt{\left(Y_{sj} - \overline{Y}_s\right)^2} \times \frac{1}{N}\sum_{j=1}^{N}\sqrt{\sum_{j=1}^{2}\left(X_{sj}^2 + Y_{sj}^2\right)} \end{aligned} \tag{5}$$

Equation (5) describes the HFSWR phase transition criterion (HPTC) proposed in this letter for the response characteristics of the HFSWR ionosphere echo-driven Duffing system, $\overline{X}$ denotes the average of X, $\overline{Y}$ denotes the average of Y.

3. Experimental Results and Analysis

Data used in this study was collected by the radar station in Weihai, Shandong Province, during the passage of typhoon "Muifa" on September 16, 2022, from 02:00 to 15:00. Typhoon "Muifa" made landfall on the Shandong Peninsula around midnight on September 16, 2022, entered the Bohai Strait at 08:00 on September 16, and made another landfall in Dalian, Liaoning at 12:00 on September 16. Data within the time interval from 08:00 to 12:40 on September 16 was selected, the typhoon center had entered the detection range of HFSWR and was located in the Bohai Strait.

It is necessary to determine the critical threshold A_c at which the motion state of the Duffing oscillator transitions from chaotic to large-scale periodic motion. As shown in (2), when $s(t) = 0$, all parameters except the driving force amplitude A are fixed and will not be altered in subsequent experiments ($m = 1, k = 0.5, \omega = 4$). Specific values of these parameters except A in (2) are not further discussed in this context. By gradually increasing the driving force amplitude A, a bifurcation diagram shown in Fig. 1 can be

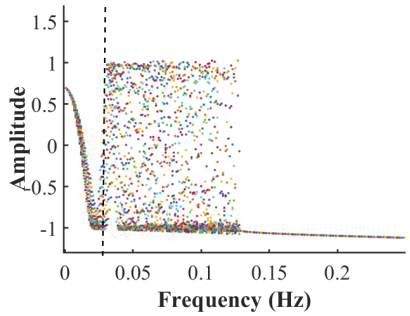

Fig. 1 A bifurcation diagram of the Duffing system designed in this approach.

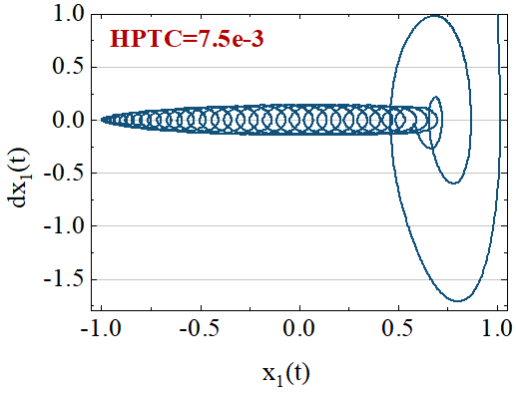

Fig. 2 Output phase diagram of the Duffing system, $A = 0.029$.

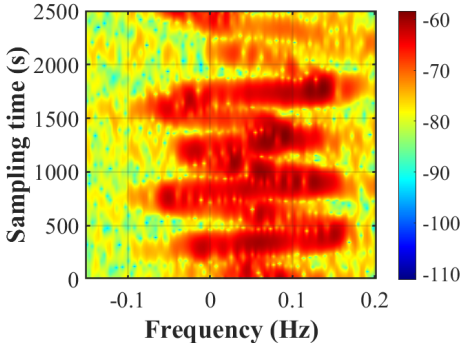

Fig. 3 The time-frequency distribution of gravity wave features.

obtained, where $A_c = 0.123$ represents the critical threshold at which the system transitions from a chaotic state to a periodic state under fixed parameter conditions. When the amplitude $A = 0.029 < A_c$, as shown in Fig. 2, the system exhibits the typical chaotic behavior of the Duffing system.

The time-frequency distribution of gravity wave features extracted from the HFSWR ionospheric echo using the short-time Fourier transform method is shown in Fig. 3. The gravity wave feature in Fig. 3 exhibits quasi-periodic sinusoidal TIDs morphology. It has been verified using the Lyapunov exponent that the time series of gravity wave feature also possess chaotic behavior. Normalized ionospheric echo pulse data with typhoon excitation at fixed range shown in Fig. 4 is used as background clutter. Ionospheric clutter data

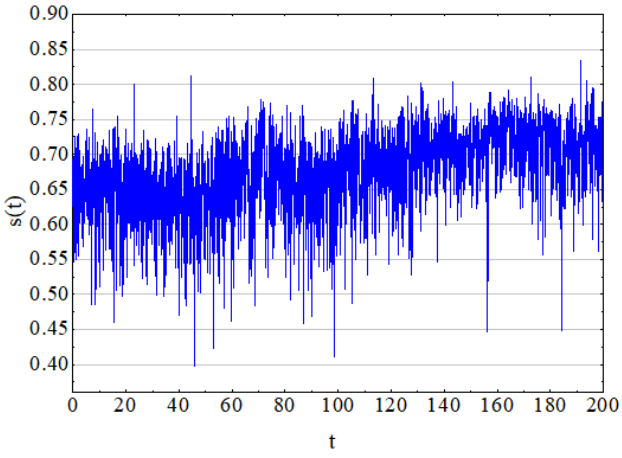

Fig. 4 Time series plot of gravity wave features without target signal.

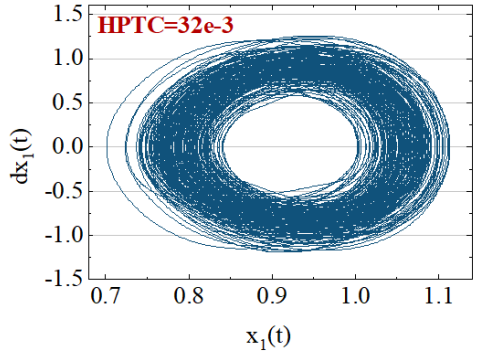

(a)

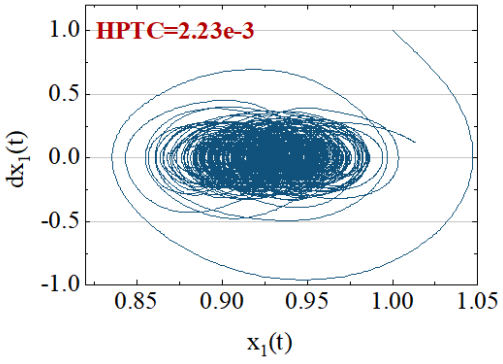

(b)

Fig. 5 The chaos detection results. (a) $s(t)$ is the time series of gravity wave features with target signal. (b) $s(t)$ is the time series of gravity wave features without target signal.

containing the target signal and data without the target are utilized as driving data. The length of the ionospheric clutter data is 3521. This experiment employs a weak signal with an amplitude of 0.026 and a length of 3521 as the target signal, the starting position of the target signal is randomly determined using a random function, and the signal-to-clutter ratio (SCR) is -31.8665dB. The chaos detection results are illustrated in Fig. 5.

It cannot be determined from the time series of gravity

wave features in the HFSWR, as shown in Fig. 4, whether it contains the target signal. However, the Duffing phase diagrams (chaos detection results) in Fig. 5 exhibit significant differences. The Duffing phase diagram of the gravity wave features containing the target signal transitions from a chaotic state to a large periodic state (see Fig. 5(a)), while the Duffing phase diagram of the gravity wave features without the target signal remains in a chaotic state (see Fig. 5(b)). HPTC provides a quantitative description of phase diagram variations in Duffing systems. Compared to the HPTC when $s(t) = 0$ in the Duffing system in Fig. 2, the HPTC varies by 326% when the $s(t)$ represents gravity wave features with the target signal, the HPTC varies by 70.27% when $s(t)$ represents gravity wave features without the target signal. The chaos detection results can confirm that the gravity wave features containing the target signal indeed caused the output phase diagram of the Duffing system to shift from a chaotic state to a large periodic state. Experimental results demonstrate the effectiveness of the proposed method in detecting target signals (including transient signals and periodic signals) with harmonic characteristics from HFSWR strong ionospheric clutter during typhoon passages.

It should be noted that the detectable target amplitudes are all different corresponding to the different Duffing system parameters A. The Duffing system parameters designed in this letter are all manually selected experimentally and the novel proposed method fails when the amplitude of the target signal is less than 0.026. Therefore, the next task is to find an adaptive method to select the optimal Duffing system parameter A with the help of the relationship between the total driving force and the critical threshold A_c to obtain a lower detectable target amplitude.

4. Conclusion

To address the difficulty of not knowing whether the target signal is contained in the ionospheric echoes when the target signal is completely flooded by the ionospheric echoes during a typhoon. This letter presents a methodology for target detection in the high-frequency surface wave radar (HFSWR) under the influence of gravity waves. The methodology begins by extracting the ionospheric time series affected by gravity waves using a preprocessing technique (Short-time Fourier transform, STFT). Additionally, by leveraging the Duffing oscillator system's sensitivity to chaotic and non-chaotic signals, the letter investigates the phase transition characteristics of the Duffing system. Furthermore, a novel HFSWR target detection approach based on chaos theory is proposed under the influence of gravity waves. Experimental results validate the feasibility of the proposed method and demonstrate its potential to advance target detection in the HFSWR field amidst challenging clutter backgrounds.

Acknowledgments

The authors would like to thank the anonymous reviewers and the Associate Editor for their helpful comments that greatly improved the presentation and quality of this letter. This work was supported in part by the National Natural Science Foundation of China under Grant 62031015 and Mount Taishan Scholar Distinguished Expert Plan 20190957.

References

[1] W. Huang, E. Gill, X. Wu, and L. Li, "Measurement of sea surface wind direction using bistatic high-frequency radar," IEEE Trans. Geosci. Remote Sensing, vol.50, no.10, pp.4117–4122, 2012.
[2] J. Walsh, S. Chen, E. Gill, and W. Huang, "High-frequency radar clutter power for mixed ionosphere-ocean propagation," 2014 16th International Symposium on Antenna Technology and Applied Electromagnetics, Victoria, Canada, no.14562768, pp.1–2, Sept. 2014.
[3] C.O. Hines, "Internal atmospheric gravity waves at ionospheric heights," Can. J. Phys., vol.38, no.7, pp.1424–1427, 1960.
[4] S. Chen, W. Huang, and E.W. Gill, "First-order bistatic high-frequency radar power for mixed-path ionosphere-ocean propagation," IEEE Geosci. Remote Sens. Lett., vol.13, no.12, pp.1940–1944, 2016.
[5] D.L. Birx, and S.J. Pipenberg, "Chaotic oscillators and complex mapping feed forward networks (CMFFNs) for signal detection in noisy environments," IJCNN International Joint Conference on Neural Networks, Baltimore, MD, USA, no.4422048, pp.881–888, Aug. 1992.
[6] H. Leung, "System identification using chaos with application to equalization of a chaotic modulation system," IEEE Trans. Circuits Syst. I, Fundam. Theory Appl., vol.45, no.3, pp.314–320, 1998.
[7] Z. Lyu, C. Yu, R. Wang, and A. Liu, "A data-driven deep neural network for modeling of ionospheric clutter in HFSWR," IEEE Geosci. Remote Sens. Lett., vol.20, no.3503805, pp.1–5, 2023.
[8] S.B. Yamgoue, B. Nana, and F.B. Pelap, "Accurate explicit analytical solutions of the duffing-harmonic oscillator equation using nonlinear time transformation," Journal of Applied Nonlinear Dynamics, vol.11, no.4, pp.951–962, 2022.
[9] B. Pokharel, M.Z.R. Misplon, W. Lynn, P. Duggins, K. Hallman, D. Anderson, A. Kapulkin, and A.K. Pattanayak, "Chaos and dynamical complexity in the quantum to classical transition," Sci. Rep., vol.8, 2018.
[10] G. Li, R. Xie, and H. Yang, "Detection method of ship-radiated noise based on fractional-order dual coupling oscillator," Nonlinear Dyn., vol.112, pp.2091–2118, 2024.
[11] C. Fu and J. Yang, "Granular classification for imbalanced datasets: A Minkowski distance-based method Algorithms," Algorithms, vol.14, no.2, p.54, 2021.
[12] X. He, X. Zhou, W. Yu, Y. Hou, and C.K. Mechefske, "Adaptive variational mode decomposition and its application to multi-fault detection using mechanical vibration signals," ISA Trans., vol.111, no.33189303, pp.360–375, 2021.